Effect of the Bubble Size and Chemical Reactions on Slag Foaming

Y. ZHANG and R.J. FRUEHAN

Slag foams have been investigated with smaller bubbles than those used in the previous studies.[5,6,7] The bubbles were generated by argon gas injection with the nozzle of multiple small orifices and by the slag/metal interfacial reaction of FeO in the slag with carbon in the liquid iron. The foam stability in terms of the foam index for a bath-smelting type of slag ($CaO-SiO_2-Al_2O_3-FeO$) was determined for different bubble sizes. The average diameter of bubbles in the foam was measured by an X-ray video technique. When the foam was generated by the slag/metal interfacial reaction at 1450 °C, it was found that the average bubble diameter varied from less than 1 to more than 5 mm as a function of the sulfur activity in the carbon-saturated liquid iron. The foam index was found to be inversely proportional to the average bubble diameter. A general correlation is obtained by dimensional analysis in order to predict the foam index from the physical properties of the liquid slag and the average size of the gas bubbles in the foam.

I. INTRODUCTION

THE growing interest in slag foaming rises in part from the worldwide activity in developing innovative iron making processes, particularly bath smelting. The bath-smelting process is designed to produce hot metal at a high specific productivity without using metallurgical coke. The process uses prereduced ore fines or pellets as the raw material, coal as the fuel and reductant, and oxygen or air injection for combustion. In this process, slag foaming needs to be controlled in order to achieve the optimum production rate without causing slopping of the liquid slag. On the other hand, a certain amount of foamed slag in the vessel is desired for promoting the transfer of heat generated by post-combustion to the bulk slag. Slag foaming is also of interest in electric are furnaces, basic oxygen steelmaking, and ladle processing, as discussed elsewhere.[1,2]

Slag foaming in steelmaking has been investigated for many years. Early studies[1,2,3] described the stability of slag foams in terms of "foam life." The measured results signified the time of the decay of a certain volume of slag foam under static conditions but could not be directly applied to predicting the height of the dynamic foam in an iron or steelmaking vessel. Recently, Ito and Fruehan[5] adopted a dynamic measurement of the foam-stability, the foam index, as the ratio of the foam height to the superficial gas velocity. In this case, the foam height is defined as the difference between the level of the surface of the foamed slag and that of the slag at rest. The foam height is usually obtained at different gas flow rates to ensure the accuracy of the experiment, and the foam index can be obtained by the slope of a plot of the foam height against the superficial gas velocity. Ito and Fruehan further measured the foam index for $CaO-SiO_2-FeO$ slags containing 30 pct FeO at temperatures from 1200 °C to 1400 °C. They also examined the effects of P_2O_5, S, and CaF_2 contents in the slag on the foam index. As the result, the foam index was correlated with the physical properties of the liquid slag by dimensional analysis. In a later study, Jiang and Fruehan[6] measured the foam index for the bath-smelting type of slags ($CaO-SiO_2-Al_2O_3-FeO$) containing less than 15 pct FeO. An improved correlation was obtained by using more accurate data for the slag viscosity, density, and surface tension in the dimensional analysis. The correlation developed is given by

$$\Sigma = 115 \frac{\mu}{\sqrt{\rho \sigma}} \qquad [1]$$

where Σ is the foam index (seconds), μ is the viscosity ($N \cdot s/m^2$), ρ is the density (kg/m^3), and σ is the surface tension (N/m). A more recent experimental investigation by Roth *et al.*[7] demonstrated that the preceding empirical equation was also followed by ladle slags ($CaO-Al_2O_3-SiO_2$) containing CaF_2 or CaS and oxygen steelmaking slags of high basicity ($CaO-SiO_2-FeO-MgO-MnO$, $CaO/SiO_2 = 3$). However, in these studies,[5,6,7] the foams were all generated by injecting argon gas into the liquid slag, and the variation in the average bubble size was small. Ito and Fruehan[5] estimated the average bubble diameter to be about 12 mm and independent of the gas flow rate by measuring the bubble formation frequency at the nozzle orifice (i.d. = 2 mm). Jiang and Fruehan[6] and Roth *et al.*[7] used a similar alumina nozzle (orifice i.d. = 1.75 mm), and the bubble size was estimated to be in the range of 5 ~ 20 mm by visual observation.

In fact, foams may have different morphologies and gas bubble cells with a large size range and, hence, very different degrees of stability. Foams have been divided into two categories: foams with spherical bubbles, called *kugelschaum* (sphere-foam), and foams with polyhedron-shaped bubbles, called *polyederschaum* (polyhedron-foam).[8,9] The first kind of foam often consists of relatively small spherical bubbles, like a "beer foam." The second kind of foam is usually composed of large bubble cells of polyhedron shape with very thin liquid lamellae separating them, like a "soap bubble foam." Consequently, the stability of the foam of a

Y. ZHANG, formerly Graduate Student and Research Associate, Department of Materials Science and Engineering, Carnegie Mellon University, is now a Senior Process Engineer with Armco Advanced Materials Company, Butler, PA 16003-0832. R.J. FRUEHAN, Professor, is with the Department of Materials Science and Engineering, Carnegie Mellon University, Pittsburgh, PA 15213.

Manuscript submitted February 9, 1993.

liquid depends not only on its intrinsic physical properties but also on the bubble size. Studies on the life of aqueous foams showed that the initial bubble size distribution was important in determining the foam stability.[10,11] The purpose of the present work is to investigate the effect of bubble size on slag foaming and to extend the previous studies by generating foams with gases resulting from the slag/metal interfacial reaction:

$$(FeO) + [C] = Fe + CO_{(g)} \qquad [2]$$

The effect of sulfur activity in the liquid metal on the formation of slag foams was also examined experimentally. A correlation relating the foam index to the physical properties of the liquid slag and the average bubble size was developed by dimensional analysis.

II. EXPERIMENTAL TECHNIQUES AND PROCEDURES

In order to examine the effect of bubble size on slag foaming, the investigators decided to vary the bubble size in a range from 1 to about 15 mm in average diameter. Therefore, slag foams were generated by argon gas injection into the liquid slag with different types of nozzles and by CO formation resulting from the slag/metal interfacial reaction. The size of gas bubbles in the slag foam was measured by the X-ray video photographic technique.

A. *Generation of Small Bubble Foams by Argon Bubbling through a Multiorifice Nozzle*

Injection of argon gas through a single-orifice (i.d. = 1.75 mm) alumina nozzle into a liquid CaO-SiO_2-Al_2O_3-FeO slag at 1500 °C would generate a foam with bubbles of approximately 10 ~ 15 mm in average diameter, as indicated by Jiang and Fruehan's work.[6] In this study, a new type of nozzle was used. It was made from an one-end-closed alumina tube (o.d. = 1/4 in. i.d. = 3/16 in.). Four small orifices with diameters less than 1 mm were machined around the perimeter of the alumina tube near its end with a diamond cutter. In the remainder of this article, this nozzle will be referred to as the multiorifice nozzle. The experimental technique and procedure to measure the foam index follow those employed by Jiang and Fruehan.[6] As illustrated in Figure 1, the foam height was measured by detecting the foam/gas interface with two molybdenum wire probes when argon gas was bubbled through the liquid at a constant flow rate. The foam index was obtained by measuring the foam height at different gas flow rates. The furnace used was heated by silicon carbide heating elements and had a 22-cm hot zone. These experiments were conducted with liquid slags of CaO/SiO_2 = 1 and contained 5 ~ 15 pct FeO at 1500 °C. After each experiment, the slag would contain on the average about 5 pct Al_2O_3 dissolved from the crucible. The average diameter of the bubbles in the foam for a typical liquid slag composition was measured in separate experiments using the X-ray video photographic equipment.

B. *Generation of Small Bubble Foams by the Slag/Metal Interfacial Reaction*

Gases resulting from the slag/metal interfacial reaction [Eq. (2)] tend to foam the slag with smaller bubbles. These

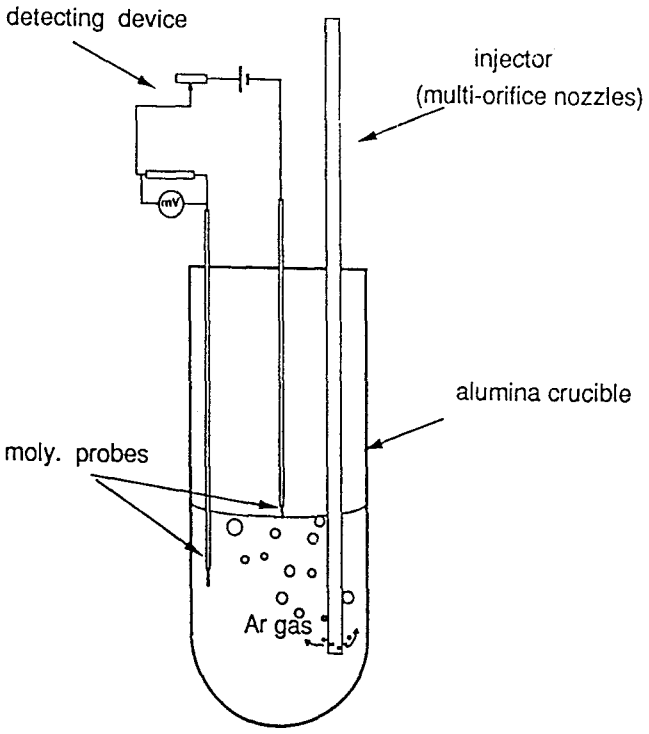

Fig. 1—Schematic diagram illustrating the measurement of the foam index with the electric contact probes for foams generated by argon gas bubbling through the slag.[6]

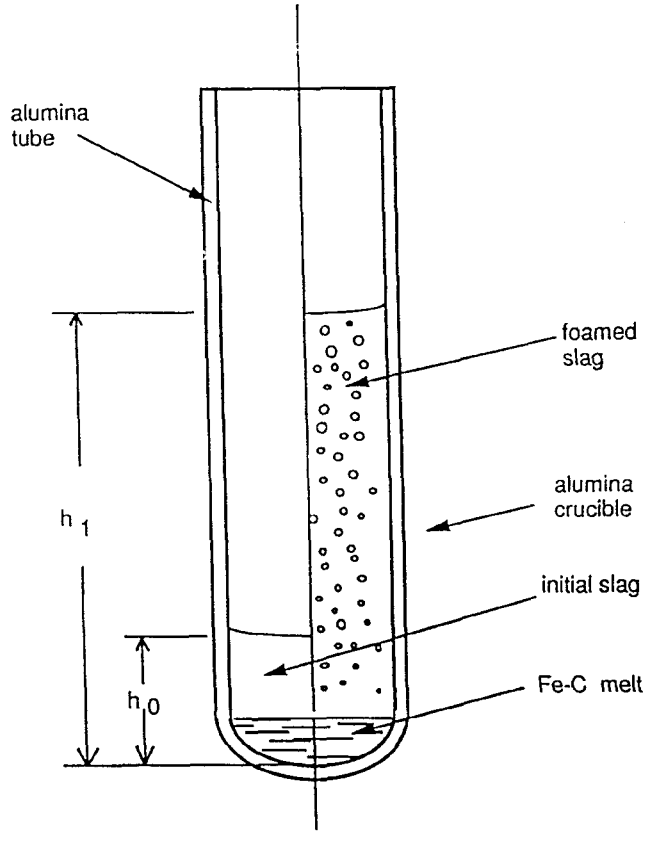

Fig. 2—Schematic diagram illustrating the measurement of the foam index for foams generated by the slag/metal interfacial reactions.

experiments were carried out in a furnace with an X-ray photographic system so that the foam image could be re-

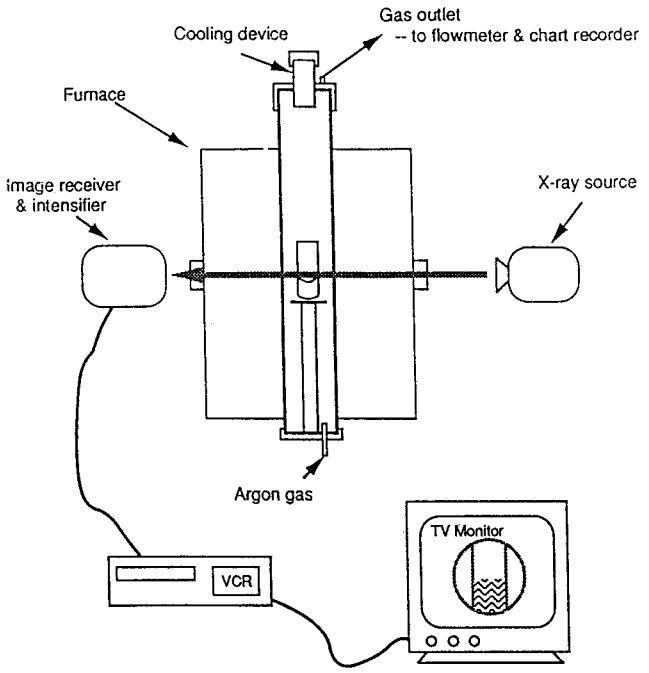

Fig. 3—X-ray video photography system.

corded while the CO gas flow rate from the reaction was measured. Figure 2 illustrates the measurement of the foam height for these experiments. About 40 g of carbon saturated Fe-C-S alloy and 60 g of slag were melted in an alumina crucible at 1450 °C. The sulfur content in the liquid metal was varied from 0.002 to 0.17 wt pct in the experiments in an attempt to control the bubble size. When the sulfur content in the liquid metal was low, the bubble size was small; therefore, a sample of the foamed slag was taken by a piece of alumina plate. The bubble size was measured from the quenched slag foam. The slag was originally composed of 40 pct CaO, 40 pct SiO_2, 5 pct FeO, and 15 pct Al_2O_3. This slag composition was further modified by using 10 pct BaO to substitute an equimolar amount of CaO. The addition of BaO was used to enhance the contrast of the X-ray image; variations in the viscosity and surface tension of the liquid slag from those of the slag with the original composition were insignificant. The foamed slag level (h_1) was measured by the X-ray video photographic equipment or estimated by the highest mark of the slag on the inner wall of the crucible after it was cooled down. The slag level before the reaction started (h_0) was calculated by the liquid slag and hot metal densities and volumes. The foam height was thus considered as ($h_1 - h_0$). This system was contained in a sealed mullite tube in a furnace with silicon carbide heating elements. The CO gas evolution rate was measured by a calibrated Matheson 8100 series digital flowmeter. The foam index was then calculated from the measured foam height and the corresponding CO gas flow rate. The estimated uncertainty in the measured foam height is about 10 ~ 15 pct.

C. *The X-Ray Video Photographic Technique*

The X-ray photographic technique described in Section B is shown schematically in Figure 3. This system was developed by I. Jimbo.[12] The X-ray radiated from the source unit is transmitted through the crucible in the furnace and is received at the other side of the furnace. The picture is then recorded by the videocassette recorder and displayed by the TV monitor. After each experiment, image analysis software (IMAGE II) was used on a MACINTOSH* personal computer to analyze the image from the playback of the recorded videotape. By calibrating the software according to the outer diameter of the crucible, the size of gas bubbles in the slag foam and the foam height were measured. For bubbles with average diameters larger than 2 mm, this technique was quite effective. The error involved in the measurement is estimated to be about 15 pct. When bubbles were too small, the X-ray image became dense and therefore made it difficult to gain a good resolution. In those cases, the bubble size was measured from the solidified foam samples. As mentioned in Section B, BaO can be added to the slag to improve the X-ray video image.

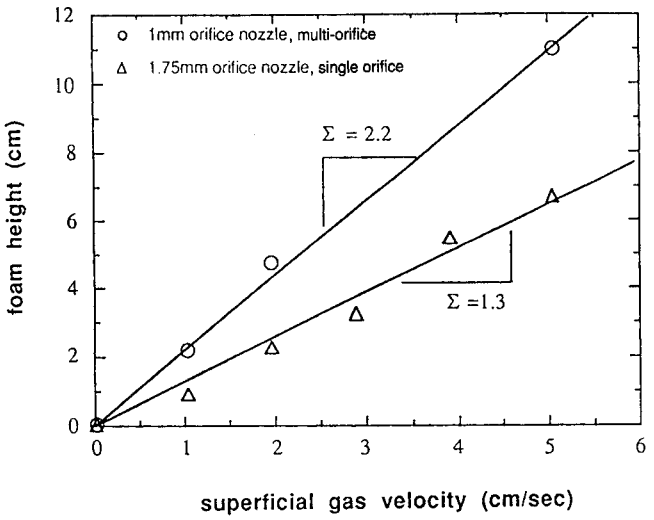

Fig. 4—Measured foam height as a function of the superficial gas velocity for the single-orifice and the multiorifice nozzles.

*MACINTOSH is a trademark of Apple Computers, Inc., Cypertino, CA.

III. EXPERIMENTAL RESULTS AND DISCUSSION

A. *Foaming Generated by Argon Gas Bubbling*

The experimental conditions chosen were the same as in Jiang and Fruehan's work.[6] In order to compare the present results with those of the previous work, the foam index was first measured using the single-orifice alumina nozzle (i.d. = 1.75 mm) to minimize any uncertainties caused by the different experimenters. Then, by separate experiments, the foam index with the new multiorifice nozzle was examined as a function of FeO content in the liquid slag. Figure 4 shows the measured foam height at different superficial gas velocities using a single-orifice nozzle and a multiorifice nozzle; the slag contained 5 pct FeO in this case. The foam height with the multiorifice nozzle increased by about 70 pct with respect to the foam height measured using the single-orifice nozzle. The foam index for foams generated

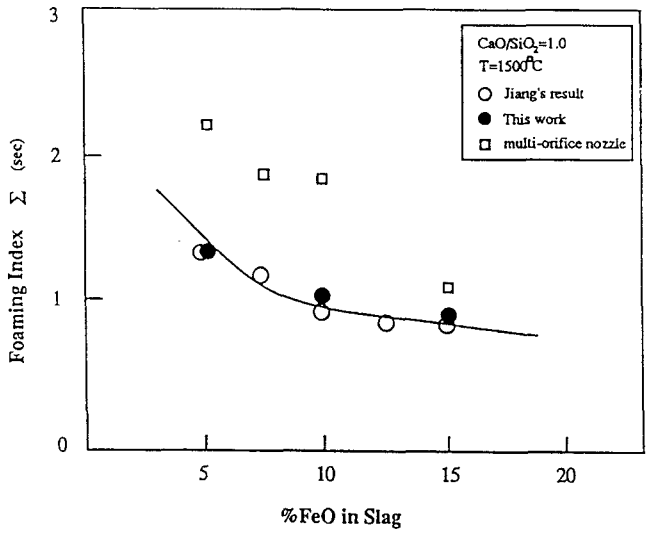

Fig. 5—Foam index measured as a function of FeO content in the slag for the single-orifice and the multiorifice nozzles.

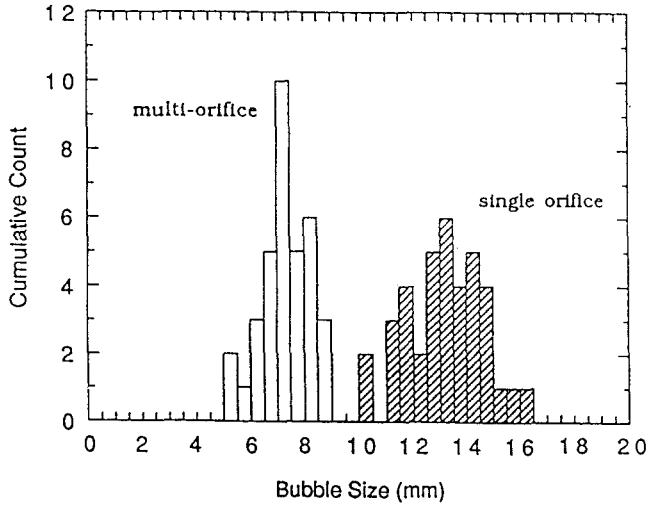

Fig. 6—Measured bubble size in the slag foams generated by gas injection.

by argon injection with the multiorifice nozzle was further examined with varying FeO content of the slag. Figure 5 shows a plot summarizing the present results along with those of Jiang and Fruehan's work. In the present research, Jiang and Fruehan's results were well reproduced with the single-orifice nozzle. The foam indices measured with the multiorifice nozzle were significantly higher than those measured with the single-orifice nozzle.

The sizes of bubbles in the slag foams generated by both the single-orifice and the multiorifice nozzles were measured using the X-ray video photographic technique. The shape of the gas bubble cells in these foams was polyhedral. The average bubble diameter was approximated by the average value of the longest and the shortest dimensions of a bubble in the two-dimensional image. The distributions of the bubble size in the foams generated by both kinds of nozzles are plotted in a bar graph, as shown in Figure 6. It can be seen that the average bubble diameter for the single-orifice nozzle case was about 13.5 mm. The average bubble size for foam generated by the multiorifice nozzle was

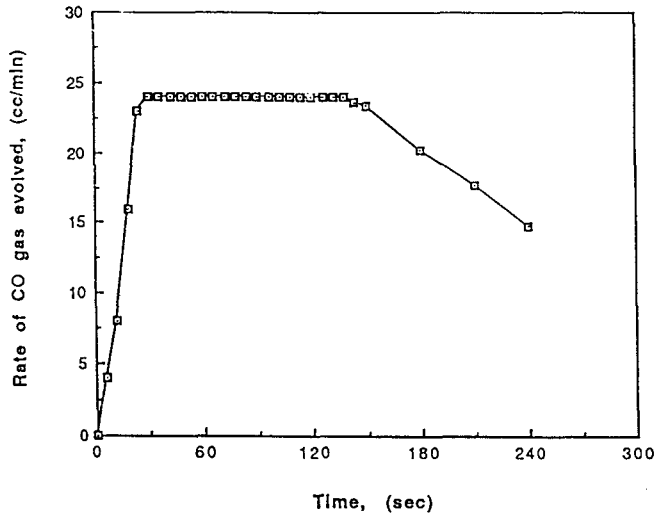

Fig. 7—CO gas evolution rate resulting from the slag/metal interfacial reactions with 5 pct FeO in the slag and at 1450 °C.

about 7.5 mm in diameter, which was about half of that measured for the single-orifice nozzle under the same experimental conditions.

B. *Foaming Generated by the Slag/Metal Interfacial Reaction*

Figure 7 shows a typical measured reaction rate in terms of the CO gas flow rate as a function of time. The sulfur content in the carbon-saturated iron was 0.002 pct in this case. It is seen that the highest gas flow rate (at about 24 cc/min) was maintained for a significant period of time, which is needed for establishing a steady-state foam height. The equivalent reaction rate is 3.07×10^{-6} moles/cm²·s. By measuring the foam height corresponding to the constant gas flow rate at the maximum reaction rate, the foam index can be determined. In this case, the foamed slag level (h_1) was 19.5 cm, and the initial slag level (h_0) was estimated at 3.5 cm. Thus, the foam height was 16 cm, which gives a foam index of 56 seconds. The measured average bubble diameter of the foam was 0.7 mm. The measurement was done by taking a foam sample using a piece of alumina scrap. Unlike the slag foam generated by argon gas injection with a nozzle, this type of foam is very much like a beer foam. It is composed of very fine spherical gas bubbles and is very stable.

The bubble size generated by nucleation at the slag/metal interface is expected to be a strong function of the interfacial tension and the contact angle between the liquid slag and metal. Hence, experiments were also carried out at different sulfur contents in the liquid metal. It was found that the average bubble size increased markedly as the sulfur content of the metal phase increased. When the liquid metal contained 0.11 wt pct of sulfur initially, the average bubble increased to 5.1 mm, as shown in Figure 8, and the maximum reaction rate decreased to 1.50×10^{-6} moles/cm²·s. The foam height was lowered to 1.5 cm. The decrease of the reaction rate is due to the presence of sulfur in the liquid metal, as discussed elsewhere in detail by Min and Fruehan.[13] In this case, the foam became a polyhedron type due to the large size of its bubble cells. It should also be noted that when the sulfur content was low, the highest

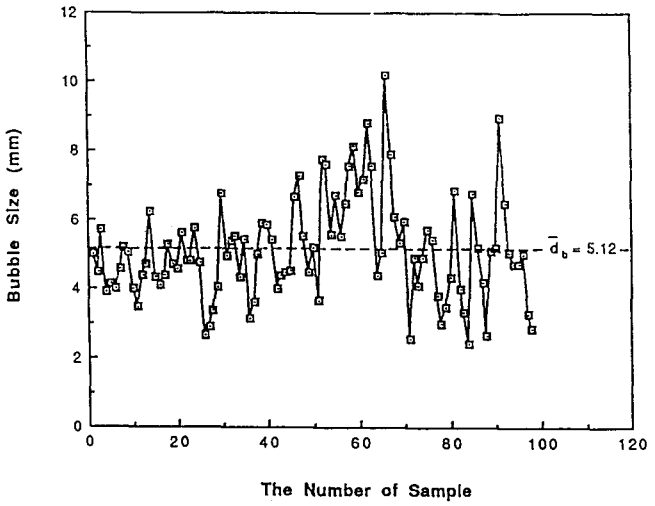

Fig. 8—Measured bubble size in the slag foams generated by the slag/metal reactions; initial sulfur content in the metal: 0.11 pct.

foam level was found to correspond to the maximum gas flow rate and therefore the initial sulfur content in the liquid metal. As the reaction rate decreased, the foam height decreased accordingly. However, when the initial sulfur content in the liquid iron was relatively high, the initial foam level that corresponded to the maximum gas flow rate (and the initial sulfur content) was not the highest, due to the larger bubble size. As a portion of sulfur transferred from the metal to the slag phase, the bubble size decreased. Consequently, the foam height would increase as a function of time, even though the reaction rate became lower. In this situation, the initial foam height was measured directly from the X-ray images.

Min and Fruehan[13] have studied the kinetics of FeO reduction in liquid slags by Fe-C droplets. The rates of the reaction measured in the present study are in agreement with their work within an order of magnitude and varied with the sulfur content in the metal, indicating that the gas/metal reaction

$$CO_{2(g)} + [C] = 2\ CO_{(g)} \qquad [3]$$

was strongly influencing the rate. However, the present experiments were conducted at a slightly higher temperature and in a completely different geometry.

Table I summarizes the results on foaming generated by the slag/metal interfacial reactions. The foam index decreased significantly as the sulfur content in the liquid metal increased. This is due to the fact that sulfur in the metal phase increased the size of the CO gas bubbles formed at the slag/metal interface. In the discussion in Section C, it can be seen that sulfur in the liquid metal decreases the interfacial tension and increases the contact angle. The contact angle is the key factor in determining the maximum size of a bubble detaching from the interface where it is nucleated.

The data for foams generated by argon gas injection also showed that the foam index decreased as the bubble size increased for a slag containing 45 pct CaO, 45 pct SiO_2, 5 pct FeO, and 5 pct Al_2O_3, as discussed in Section B. The physical properties of this slag at 1400 °C do not differ much from those of the slag used in the slag/metal reaction experiments (34 pct CaO, 37.5 pct SiO_2, 5 pct FeO, 14 pct Al_2O_3, and 9.5 pct BaO). Therefore, the foam indexes measured for the single-orifice nozzle and the multiorifice nozzle at 1500 °C were extrapolated to 1400 °C using Jiang and Fruehan's correlation (Eq. [1]) based on their dimensional analysis.[6] The ratio of the foam indexes at two different temperatures was assumed to be equal to the ratio of the property term on the right-hand side of Eq. [1]. $\mu/\sqrt{\rho\sigma}$, evaluated at these temperatures. Hence, the foam index is plotted against the reciprocal of the average bubble diameter in Figure 9, for which foams were generated either by argon injection or the slag/metal interfacial reaction. The foam index is inversely proportional to the bubble size for slags having the same physical properties. A comprehensive dimensional analysis that will include the bubble size as an independent variable will be given in Section IV.

C. *Effect of Sulfur in Liquid Metal on the Bubble Size*

As shown in Table I, the size of the bubbles formed at the slag/metal interface varied with the sulfur content in the metal phase. During the experiment, sulfur was transferred from the metal phase to the slag phase. The initial and final sulfur contents in the metal phase and the final sulfur content in the slag phase were analyzed. The final carbon content of the metal was also analyzed. Table II is a mass balance of sulfur for a typical experiment assuming the slag phase initially contained no sulfur. As sulfur was transferred from the metal phase, the bubble size in the slag foam decreased. Two bubble sizes were therefore measured in accordance with the initial and the final sulfur contents of metal, respectively. Figure 10 shows the average bubble diameter in the slag foams as a function of sulfur content in the liquid iron. Ogawa *et al.*[14] also measured the bubble size at different sulfur contents. If their sulfur content was measured from the metal phase, then their results agree well with the present data, as shown in Figure 10. Knowing the carbon content in the metal, the activity of sulfur for the 1 wt pct standard state can be estimated. In Figure 11, the average bubble diameter in the slag foams is plot-

Table I. Effect of Sulfur Content in Metal Phase on the Bubble Size in Foams Generated by the Slag/Metal Reactions and the Foam Index

$[Pct\ S]_{initial}$	$[Pct\ S]_{final}$	Reaction Rate (moles/cm²·s)	Average Bubble Diameter (mm)	Foam Height (cm)	Foam Index (s)
0.002	0.002	3.07×10^{-6}	0.70	16	56
0.064	0.032	2.54×10^{-6}	1.7*	8.8	25
0.054	0.015	2.70×10^{-6}	3.00	2.5	7.5
0.110	0.056	2.07×10^{-6}	5.10	1.5	5.7
0.170	0.071	1.50×10^{-6}	5.40	1.1	5.75

*This experiment was conducted under carbon saturation; bubble size corresponded to the final sulfur content.

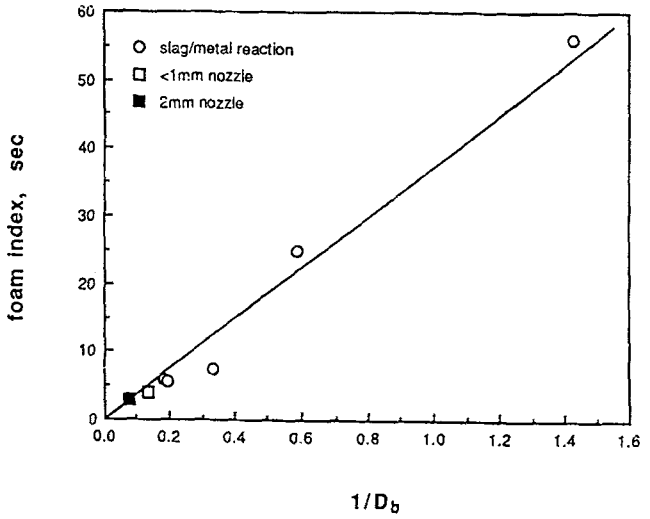

Fig. 9—The foam index as a function of the reciprocal of the average bubble diameter.

Table II. Mass Balance of Sulfur for a Typical Experiment, with 0.054 Percent Initial Sulfur Content in Metal (the Weights of Metal and Slag are Assumed to be Constant)

Phase	Total Weight (g)	Initial Sulfur Content (Pct)	Final Sulfur Content (Pct)	Net Change (g)
Slag	60.00	0.0	0.056	0.034
Metal	42.43	0.054	0.015	0.017

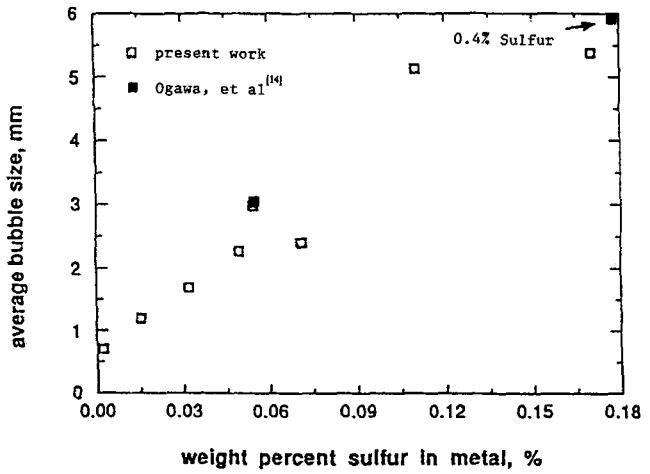

Fig. 10—Average bubble diameter in the foams generated by the slag/metal reactions as a function of the sulfur content in the liquid metal.

ted *vs* the activity of sulfur relative to 1 wt pct in the liquid iron.

According to Kojima,[15] the effect of a small amount of sulfur in the slag phase on its surface tension is negligible for a basic ($CaO/SiO_2 \geq 1$) $CaO\text{-}SiO_2\text{-}Al_2O_3$ slag system. The final sulfur content in the slag in the present work was generally less than 0.07 pct. Therefore, the interfacial tension and the contact angle can be assumed to depend only on the sulfur content in the metal phase. The effect of sulfur activity in the metal on the contact angle between the liquid metal and a $CaO\text{-}SiO_2\text{-}Al_2O_3\text{-}FeO$ slag at 1550 °C, given by Cramb and Jimbo,[16] is shown in Figure 12; the higher

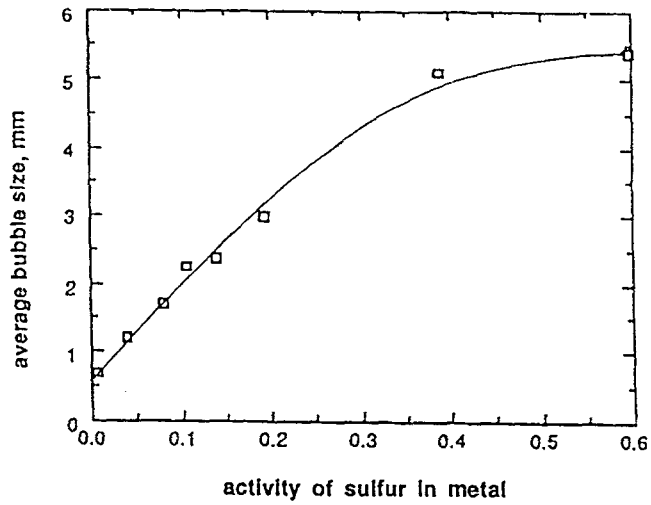

Fig. 11—Average bubble diameter as a function of sulfur activity in 1 wt pct standard state in the metal phase.

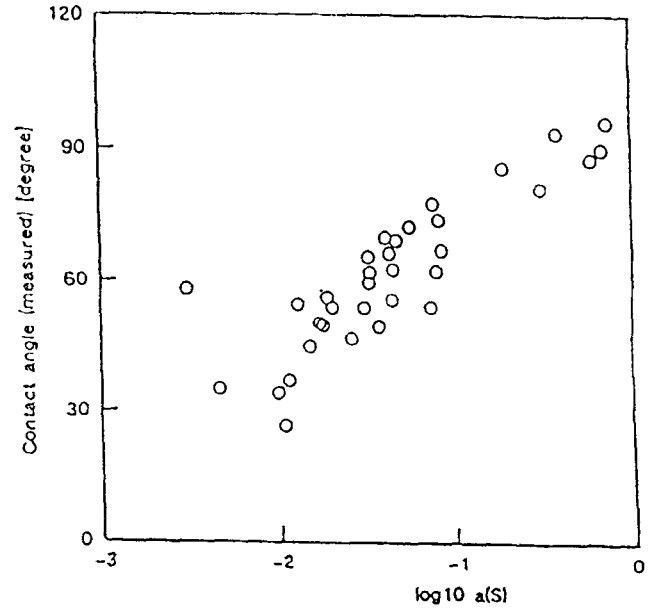

Fig. 12—Contact angle between the liquid slag and metal as a function of the sulfur activity (1 wt pct standard state) in the metal phase, after Cramb and Jimbo.[16]

the sulfur activity in the liquid iron, the higher the contact angle.

In the work by Ogawa and Tokumitsu,[17] slag foaming due to CO gas formation by interfacial reaction between carbon-saturated iron and a $CaO\text{-}SiO_2\text{-}Al_2O_3\text{-}FeO\text{-}MgO$ slag at 1500 °C was also investigated. In their investigation, the slag without FeO and the carbon-saturated iron were first melted in a graphite crucible. Then sulfur was added to the liquid slag as FeS. The FeO reagent was charged into the slag after the FeS addition. In the case where no sulfur was added, the bubble diameter was less than 1 mm. When the sulfur addition was 1 wt pct of the total slag, the size of the CO gas bubbles was more than 6 mm in average diameter for the slag containing 5 pct FeO. These findings also agree with the present results. However, the present study demonstrates that it is the sulfur in the metal phase, not the sulfur in the slag phase, that is responsible for the

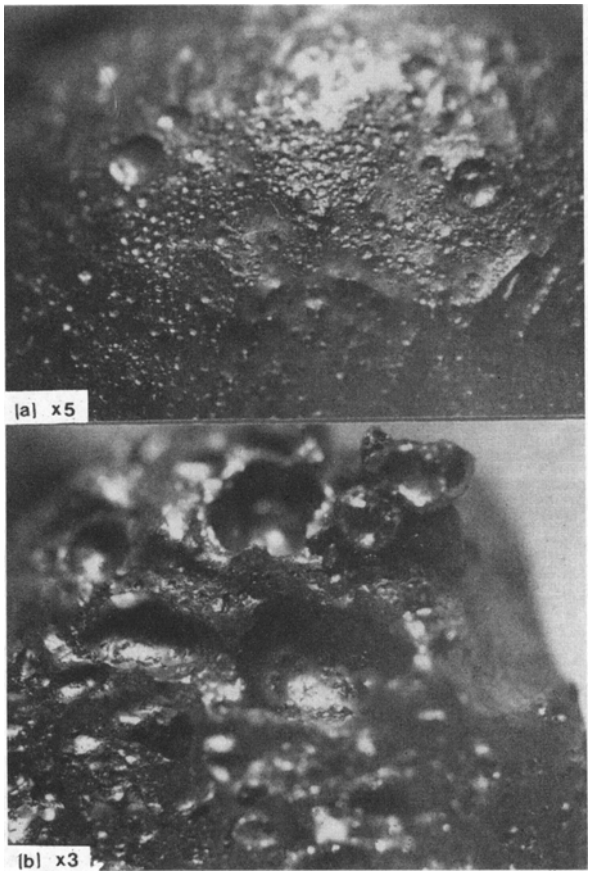

Fig. 13—Lenticular-shaped cavities on the surface of the metal samples taken after the experiments with (*a*) 0.002 pct and (*b*) 0.1 pct initial sulfur content.

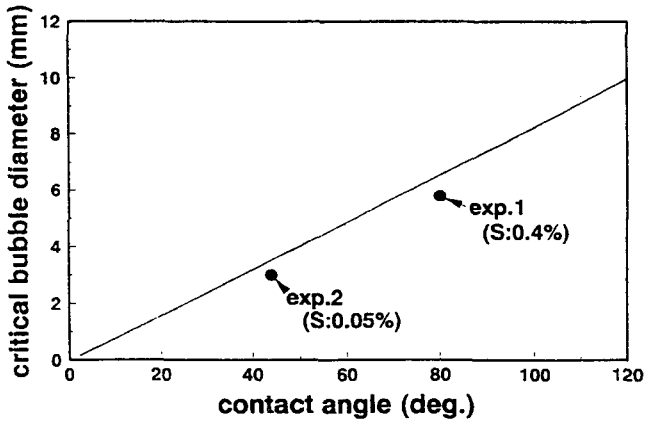

Fig. 14—The effect of the metal/slag contact angle on the bubble size, from Ogawa *et al.*[14]

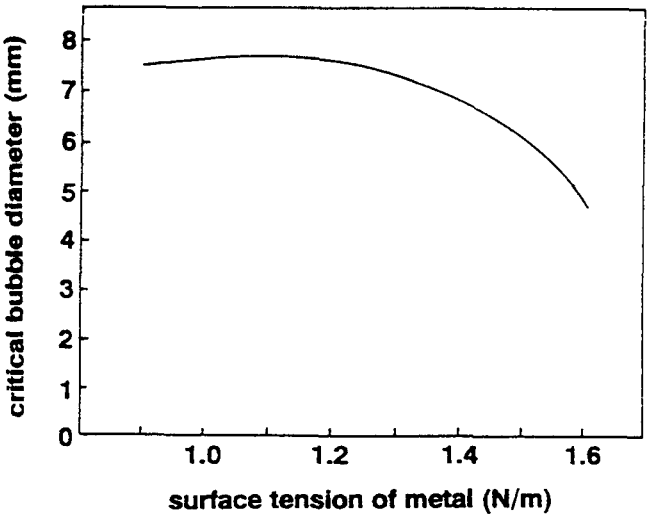

Fig. 15—The effect of the surface tension of hot metal on the bubble size, assuming that surface tension of slag and the metal/slag interfacial tension are constant.[14]

increase in the size of CO gas bubbles formed at the slag/metal interface due to the chemical reaction. Ito and Fruehan[5] also showed experimentally that the addition of CaS up to 2 wt pct of sulfur into a $CaO\text{-}SiO_2\text{-}FeO$ slag at 1400 °C did not decrease the foam index significantly. It can be speculated that in Ogawa and Tokumitsu's work, the sulfur was transferred from the slag phase to the metal phase as the result of sulfur partition during the experiment.

In the present work, the Fe-C-S metal sample was photographed after the experiment. Figure 13 shows pictures of two samples that initially contained 0.002 and 0.1 pct sulfur, respectively. Various-sized craters were found on the surfaces of these samples, which may indicate CO bubble formation at the slag/metal interface. The size of the craters on the 0.1 pct sulfur sample was significantly larger than that on the other sample, which contained 0.002 pct sulfur. Kozakevitch[18] also observed lenticular-shaped cavities on iron droplet samples taken from the emulsified slag in an actual steelmaking process. These observations may reflect the bubble formation and growth at the slag/metal interface at the temperature that the reaction occurred and also indicate that the bubble size was determined by the interfacial phenomena.

The size of a CO gas bubble detaching from the slag/metal interface after the growth may be considered to be governed by the balance between the buoyancy force and the surface-tension force. Zhang[19] theoretically calculated the bubble size as a function of the contact angle by assuming that the gas/slag and the gas/metal interfaces are spherical shaped. It was demonstrated that the maximum size of a bubble formed at the slag/metal interface increases as the contact angle increases. Furthermore, the contact angle can be increased by increasing the sulfur content in the metal phase. This is because, as discussed in this section, sulfur in the metal phase decreases the surface tension of the hot metal and, therefore, decreases the interfacial tension and increases the contact angle.

Recently, Ogawa *et al.*[14] studied the configuration and the size of a gas bubble formed at the slag/metal interface by solving Laplace's equation of capillary. The size of the bubble detaching from the interface is determined by the static balance of the three interfacial tensions (slag/gas: σ_s; metal/gas: σ_m; and metal/slag: σ_{ms}) and the static pressure. A similar numerical technique was also discussed by Terashima *et al.*[20] They have shown that the calculated bubble size using spherical approximation was larger than that obtained by numerical solution of the Laplace equation of capillary; the latter was in good agreement with measured bubble size in the water/mercury system.

Figures 14 and 15 are from Ogawa *et al.*[14] it can be seen that the maximum bubble diameter that can be stable at the

Table III. Comparison of the Calculated Bubble Size by Ruff's Model with the Measured Data

	$CaO-SiO_2-FeO-Al_2O_3$ 1500 °C (Orifice Diameter = 1.75 mm)	$CaO-SiO_2-FeO$ 1300 °C (Orifice Diameter = 2 mm[5])	$CaO-SiO_2-FeO-Al_2O_3$ 1500 °C (Orifice Diameter = 1 mm)
Measured (mm)	13.5	12.0	7.8
Calculated (mm)	12.1	11.4	8.5

slag/metal interface formed from the interfacial reaction increases as the contact angle increases. The bubble diameter also increases as the metal surface tension decreases. These theoretical predictions are excellent explanations of the experimental results of the present work. However, it must be noted that the slag/gas, metal/gas, and metal/slag interfacial tensions (or the contact angle) cannot be varied independently in reality; this was ignored by Ogawa *et al.* Therefore, Figures 14 and 15 only demonstrate the trends of the variations.

It should also be mentioned that the size of the bubbles detaching from the interface may be affected by the turbulent fluid flow induced by the local surface-tension gradient due to the temperature difference,[21] as well as the chemical reactions.[22] These effects reduce the bubble size but are difficult to predict.

IV. DIMENSIONAL ANALYSIS

The previous correlation (Eq. [1]) developed by dimensional analysis used to predict the foam index should be reconsidered to include the average bubble diameter as an independent variable. In reality, the bubble size is not completely an independent variable. For the case where the bubbles were formed by gas dispersion from an orifice, the average diameter may depend on the liquid viscosity, surface tension, nozzle geometry, and gas flow rate. However, one can always vary the bubble size by changing the orifice geometry while keeping the physical properties of the liquid constant. Therefore, in the following analysis, the bubble diameter will be considered independent of the physical properties of the slag.

Based on the knowledge of the physical phenomena, the foam index Σ can be expressed as a function of all the independent variables.

$$f(\Sigma,\sigma,\mu,D_b,\rho,g) = C \quad [4]$$

where C is a constant. The definitions and the dimensions of the variables are as follows:

Σ = foam index (seconds),
μ = slag viscosity (N·s/m^2),
σ = slag surface tension (N/m),
ρ = slag density (kg/m^3),
g = gravitational accceleration (m/s^2),
D_b = average bubble diameter (m).

The following three dimensionless groups can be obtained based on the principle of dimensional homogeneity:

$$\pi_1 = \frac{\Sigma\mu g}{\sigma} \quad [5]$$

$$\pi_2 = \frac{\mu^4 g}{\sigma^3 \rho} \quad [6]$$

$$\pi_3 = \frac{\rho^2 D_b^3 g}{\mu^2} \quad [7]$$

The dimensionless group π_1 is denoted as N_Σ. Further, π_2 and π_3 are recognized as Morton's number (Mo) and Archimedes number (Ar), respectively. The Morton's number signifies the ratio of the viscous force to the surface tension force, and the Archimedes number describes the ratio of the buoyancy force to the viscous force. Therefore, the following equation can be written:

$$N_\Sigma = C \cdot \mathrm{Mo}^\alpha \mathrm{Ar}^\beta \quad [8]$$

where α and β are exponential coefficients.

There are experimental results by Ito and Fruehan,[5] Jiang and Fruehan,[6] and Roth *et al.*[7] of the foam index for different slag systems. Unfortunately, the exact measurements of the bubble size are not available for most of their results. However, the range of the variation of the bubble size was small since the diameters of the nozzles used in these studies were almost the same. Brimacombe *et al.*[23] recommended Ruff's model[24] to predict the size of the bubble formed by dispersing gases through an orifice into liquid slags. Table III compares the calculated values of the bubble size with those measured by experiments that are available. The bubble sizes predicted by the model agree well with the experimental results. This model was then used to estimate the bubble sizes for the experiments by Ito and Fruehan, Jiang and Fruehan, and Roth *et al.*, where the bubble sizes in the slag foam were not given.

The estimation of the slag physical properties follows the methods used by Jiang and Fruehan.[6] The density was calculated from the slag molar volume, which was estimated by the addition of the partial molar volumes of each slag component. The partial molar volumes are assumed to be equal to the molar volume of the pure components, which are given in the literature.[25] The estimation of the slag surface tension was also based on the addition of the partial molar quantities of each slag component. The partial molar surface tensions are also assumed to be equal to the molar surface tensions of the pure oxides, which are also found in the literature.[25] The estimation of slag viscosity is based on Urbain's model.[26] Tables IV and V summarize the slag physical properties, measured average bubble diameters, and the foam indexes for the present experimental investigation where the slag foam was generated both by gas injection and the slag/metal interfacial reaction.

The dimensionless numbers N_Σ, Mo, and Ar were calculated from the measured foam index, the average bubble diameter, and the slag physical properties. By taking the

Table IV. List of Data for the Multiorifice Nozzle Experiments

(FeO) (Wt Pct)	Viscosity (N/m·s)	Surface Tension (N/m)	Density (kg/m³)	Bubble Diameter (mm)	Foam Index (s)
5	0.398	0.463	2743	7.8	2.20
07.5	0.375	0.467	2777	7.8	1.85
10	0.354	0.471	2812	7.8	1.80
15	0.318	0.480	2885	7.8	1.20

Table V. List of Data for the Slag/Metal Reaction Experiments*

Initial Sulfur Content (Wt Pct)	Average Bubble Diameter (mm)	Foam Index (s)
0.002	0.7	56
0.064	1.7	25
0.054	3.0	7.5
0.110	5.1	5.7
0.170	5.4	5.75

*Slag viscosity: 1.24 N/m·s; slag surface tension: 0.467 N/m; slag density: 3030 kg/m³.

logarithm of both sides of Eq. [8] and carrying out a multiple component linear regression analysis, coefficients α and β and the constant C were obtained. The final result of the dimensional analysis is described by the following equation:

$$N_\Sigma = 900 \cdot \mathrm{Mo}^{0.39}\mathrm{Ar}^{-0.28} \quad [9]$$

Considering experimental error, the coefficients can be approximately taken as 0.4 and −0.3. The gravitational acceleration is 9.8 m/s², so the foam index is given by

$$\Sigma = 115 \frac{\mu^{1.2}}{\sigma^{0.2}\rho D_b^{0.9}} \quad [10]$$

Figure 16 shows the plot of ln (N_Σ) *vs* ln ($\mathrm{Mo}^{0.4}\mathrm{Ar}^{-0.3}$). The slope of the line that fits to the data points in this graph is unity. Figure 17 compares the foam index calculated by Eq. [10] and the experimental results. The agreement is acceptable. Equation [10] indicates that the foam index is proportional to the average bubble diameter raised to the −0.9 power, which is close to the inverse proportionality that has been demonstrated in Section III C.

In the preceding dimensional analysis, the average bubble diameter was taken as an independent variable. In reality, it would also depend on the physical properties of the slag and other conditions related to the formation of the bubble, such as the orifice diameter if the bubble is formed by gas injection, or the slag/metal contact angle if the bubble is formed by slag/metal reactions. Comparing Eq. [10] with Eq. [1], it is found the foam index becomes more dependent on the viscosity and density, but less dependent on the surface tension in Eq. [10]. In previous investigations, the effect of the bubble size was not considered and was assumed constant. However, the bubble size would also have varied with the physical properties since the orifice diameter was constant. In Ruff's model, the dependence of the bubble diameter on the surface tension, viscosity, and density is complicated. However, for relatively low gas flow rates, the bubble diameter is proportional to the viscosity to the 0.25 power and to the density to the −0.25

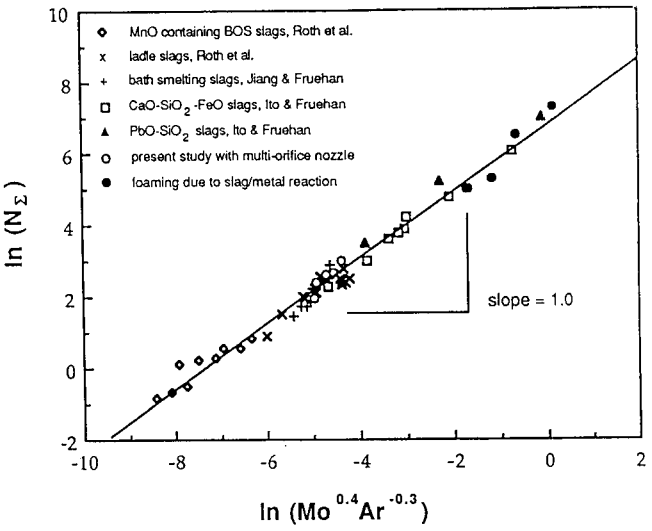

Fig. 16—The result of the dimensional analysis considering the effect of the bubble size. $N_\Sigma = \Sigma\mu g/\sigma$; $\mathrm{Mo} = \mu^4 g/\sigma^3\rho$; and $\mathrm{Ar} = \rho^2 D_b^3 g/\mu^2$

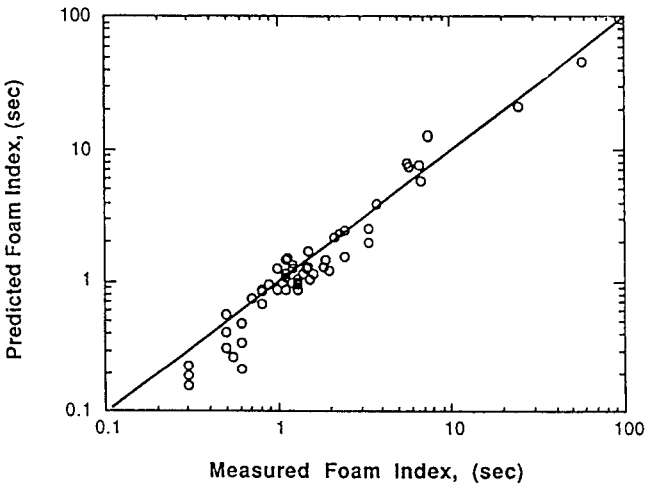

Fig. 17—Comparison between the measured foam index and that predicted by the correlation obtained from the dimensional analysis.

power and independent of the surface tension for viscous liquids.[23] For a liquid of low viscosity, the bubble diameter is proportional to the surface tension to the 1/3 power, to the density to the −1/3 power, and to the viscosity to the zeroth power.[23] Considering these effects of the slag physical properties on the diameter of the gas bubble formed by injection through an orifice, Eq. [10] would become similar to the form of Eq. [1], if the bubble size is related to the slag physical properties and the nozzle orifice diameter. This is because, in developing Eq. [1], the bubble size was assumed to be constant.

V. CONCLUSIONS AND SUMMARY

Slag foams with smaller bubbles were generated by argon gas injection into the liquid slag with a multiorifice nozzle and by the slag/metal interfacial reaction between the carbon in liquid iron and FeO in the slag. It was found that slag foams can have very different structures. Foams with very fine bubbles have spherical bubble cells and are very stable. Foams with large bubbles have polyhedral bubble cells and are less stable. The foam index was found to be approximately inversely proportional to the average bubble diameter.

The size of bubbles in foams generated by the slag/metal interfacial reaction depends on the sulfur activity in liquid metal. This is because the maximum bubble size detaching from the interface is determined by a balance between the buoyancy and interfacial tension and therefore depends on the contact angle. Sulfur, which is a strong surface active element in liquid iron, increases the contact angle, resulting in larger bubbles and less stable foams.

A general correlation is obtained by dimensional analysis that can be used to predict the foam index for the liquid slag as a function of its physical properties and the size of the bubbles in the slag foam. It was found that the foam index increases with the viscosity, decreases with the density and bubble diameter, and is relatively independent of the surface tension.

ACKNOWLEDGMENTS

The authors wish to acknowledge the AISI Direct Steelmaking Project funded 77 pct by the Department of Energy for partial support of the research and to NSF (MSM 8713961) for significant support and to the Center for Iron and Steelmaking Research and to its member companies for supporting Y. Zhang. The authors also wish to thank Dr. I. Jimbo for his assistance in the X-ray experiments.

REFERENCES

1. C.F. Cooper and J.A. Kitchener: *J. Iron Steel Inst.*, 1959, Sept., p. 48–55.
2. J.H. Swisher and C.L. McCabe: *Trans. TMS AIME*, 1964, vol. 230, p. 1669–1675.
3. S. Hara, M. Ikuta, M. Kitamura, and M. Ogino: *Tetsu-to-Haganeá*, 1983, vol. 69, p. 1152–59 (in Japanese).
4. P. Kozakevitch: *J. Met.*, 1969, vol. 21, p. 57–67.
5. K. Ito and R.J. Fruehan: *Metall. Trans. B*, 1989, vol. 20B, p. 509–514.
6. R. Jiang and R.J. Fruehan: *Metall. Trans. B*, 1991, vol. 22B, p. 481–489.
7. R. Roth, R. Jiang, and R.J. Fruehan: *Ironmaking and Steelmaking*, 1992, Nov., pp. 55-63.
8. E. Manegold: *Schaum, Chemie und Technik Verlagsgesellschaft*, Heidelberg, 1953.
9. S. Ross and I.D. Morrison: *Colloidal Systems and Interfaces*, John Wiley & Sons, New York, NY, 1988, p. 294.
10. A. Monsalve and R.S. Schechter: *J. Colloid Interface Sci.*, 1984, vol. 97, p. 327–335.
11. S. Ross: *J. Phys. Chem.* 1943, vol. 47, p. 266–277.
12. I. Jimbo: Carnegie Mellon University, Pittsburgh, PA, private communication, 1992.
13. D.-J. Min and R.J. Fruehan: *Metall. Trans. B*, 1992, vol. 23B, p. 29–37.
14. Y. Ogawa, D. Huin, Henri Gaye, and N. Tokumitsu: *ISIJ International*, vol. 33 (1993), p. 224–232.
15. Y. Kojima: *Trans. Iron Steel Inst. Jpn.*, 1971, vol. 11, p. 349–354.
16. A.W. Cramb and I. Jimbo: *Steel Res.*, 1989 (3/4), vol. 60, p. 157–165.
17. Y. Ogawa and N. Tokumitsu: *Proc. of 6th International Iron and Steel Congress*, ISIJ, Nagoya, Japan, 1990, p. 147–152.
18. P. Kozakevitch: in *Kinetics of Metallurgical Processes in Steelmaking*, W. Dahl, K.W. Lange, and D. Papamantellos eds., Düsseldorf, 1975, p. 513–533.
19. Y. Zhang: Ph.D. Thesis, Carnegie Mellon University, Pittsburgh, PA, 1992.
20. H. Terashima, T. Nakamura, K. Mukai, and D. Izu: *J. Jpn. Inst. Met.*, 1992, vol. 56, p. 422–429 (in Japanese).
21. A.K. Chesters: *International J. of Multiphase Flow*, 1978, vol. 4, p. 279–302.
22. K. Mukai: US-Japan Joint Seminar, Fundamentals of Bath Smelting and Clean Steel Production, Myrtle Beach, October 7–9, 1991.
23. J.K. Brimacombe, K. Nakanishi, P.E. Anagbo, and G.G. Richards: *Elliott Symposium*, 1990, June 10-13, 1990, Cambridge, MA, MIT, p. 304–72.
24. K. Ruff: *Chem.-Ing.-Tech.*, 1972, vol. 44, p. 1360.
25. K.C. Mills and B.J. Keene: *Int. Mater. Rev.* 1987, vol. 32 (1/2), p. 105–110.
26. G. Urbain: *Steel Res.*, 1987, vol. 58 (3), p. 111–16.